Spontaneous and stimulated emission spectroscopy of a Nd^{3+}-doped phosphate glass under wavelength selective pumping

I. Iparraguirre,[1] J. Azkargorta,[1] R. Balda,[1,2] K. Venkata Krishnaiah,[3] C.K. Jayasankar,[3] M. Al-Saleh,[1] and J. Fernández[1,2,*]

[1]*Departamento de Fisica Aplicada I, Escuela Superior de Ingenieria, Universidad del Pais Vasco UPV/EHU, Alda. Urquijo s/n 48013 Bilbao, Spain*

[2]*Materials Physics Center CSIC-UPV/EHU and Donostia International Physics Center, 20018 San Sebastian, Spain*

[3]*Department of Physics, Sri Venkateswara University, Tirupati – 517 502, India*

**wupferoj@bi.ehu.es*

Abstract: The influence of the host matrix on the spectroscopic and laser properties of Nd^{3+} in a K-Ba-Al phosphate glass has been investigated as a function of rare-earth concentration. Site-selective time resolved laser spectroscopy and stimulated emission experiments under selective wavelength laser pumping show the existence of a very complex crystal field site distribution of Nd^{3+} ions in this glass. The peak of the broad stimulated $^4F_{3/2} \rightarrow {}^4I_{11/2}$ emission shifts in a non monotonous way up to 3 nm as a function of the excitation wavelength. This behavior can be explained by the relatively moderate inter-site energy transfer among Nd^{3+} ions found in this system and measured by using fluorescence line narrowing spectroscopy. The best slope efficiency obtained for the laser emission was 40%.

OCIS codes: (140.3530) Lasers, Neodymium; (300.6500) Spectroscopy, time resolved; (160.5690) Rare earth doped materials

References and links

1. F. J. Duarte, *Tunable laser applications* (CRC, New York, 2009).
2. M. J. Weber, "Science and technology of laser glass," J. Non-Cryst. Solids **123**(1-3), 208–222 (1990).
3. M. J. Weber, "Fluorescence and glass lasers," J. Non-Cryst. Solids **47**(1), 117–133 (1982).
4. L. A. Riseberg, "Laser-Induced Fluorescence-Line-Narrowing Spectroscopy of Glass: Nd," Phys. Rev. A **7**(2), 671–678 (1973).
5. M. J. Weber, "Laser Excited Fluorescence Spectroscopy in Glass," in *Laser Spectroscopy of Solids*, W.M. Yen and P.M. Selzer, eds. (Springer, Berlin, 1981), pp. 189–239.
6. S. A. Brawer and M. J. Weber, "Observation of fluorescence line narrowing, hole burning, and ion-ion energy transfer in neodymium laser glass," Appl. Phys. Lett. **35**(1), 31–33 (1979).
7. J. H. Campbell and T. I. Suratwala, "Nd-doped phosphate glasses for high-energy/high-peak-power lasers," J. Non-Cryst. Solids **263&264**(1-2), 318–341 (2000).
8. R. Balakrishnaiah, P. Babu, C. K. Jayasankar, A. S. Joshi, A. Speghini, and M. Bettinelli, "Optical and luminescence properties of Nd^{3+} ions in K–Ba–Al-phosphate and fluorophosphate glasses," J. Phys. Condens. Matter **18**(1), 165–179 (2006).
9. W. F. Krupke, "Induced emission cross-sections in neodymium laser glasses," IEEE J. Quantum Electron. **QE-10**(4), 450–457 (1974).
10. R. Balda, J. Fernández, M. Sanz, A. de Pablos, J. M. Fdez-Navarro, and J. Mugnier, "Laser spectroscopy of Nd^{3+} ions in GeO_2-PbO-Bi_2O_3 glasses," Phys. Rev. B **61**(5), 3384–3390 (2000).
11. T. T. Basiev, V. A. Malyshev, and A. K. Prhvuskii, "Spectral Migration of Excitations in Rare-Earth Activated Glasses," in *Spectroscopy of Solids Containing Rare Earth Ions*, A.A. Kaplyanskii and R.M. Macfarlane, eds. (North-Holland, Amsterdam, 1987), pp. 275–341.
12. L. M. Lacha, R. Balda, J. Fernández, and J. L. Adam, "Time-resolved fluorescence line narrowing spectroscopy and fluorescence quenching in Nd^{3+}-doped fluoroarsenate glasses," Opt. Mater. **25**(2), 193–200 (2004).
13. R. Balda, M. Sanz, J. Fernández, and J. M. Fdez-Navarro, "Energy transfer and upconversion processes in Nd^{3+}-doped GeO_2–PbO–Nb_2O_5 glass," J. Opt. Soc. Am. B **17**(10), 1671–1677 (2000).

#150021 - $15.00 USD Received 27 Jun 2011; revised 8 Sep 2011; accepted 15 Sep 2011; published 22 Sep 2011

1. Introduction

The search for new rare earth (RE)-doped laser glass matrices is still a challenge of great interest for a wide range of industrial applications as well as for scientific basic research. For example, glass fiber lasers and amplifiers emitting at selected wavelengths in the continuous or pulsed time domain are of paramount importance for bioimaging, optical biosensors, light activated therapy, and broadband telecommunications [1].

As it is well known the reason why RE ions have been commonly used as probes for local ordering [2] is the close relation among the spectroscopic properties of RE-doped glasses and the local structure and bonding at the ion site. In a glass the lack of long range order produces the observed inhomogeneous spectral broadening of the RE spectra. For some applications this behavior may offer some advantages concerning laser tunability and, moreover, the possibility of controlling the laser parameters by varying the chemical composition of the host glass.

From a more fundamental point of view, the inhomogeneous nature of the crystal field (CF) being seen by the RE ions in a glass, may seriously affect the optimum energy extraction [3] and also the peak emission wavelength at which the stimulated emission occurs when a spectrally narrow pump is used. In order to have a clear picture about these complexities, the distribution of the spectroscopic parameters from site to site must be considered. These effects can either be observed and quantified by fluorescence line-narrowing (FLN) spectroscopy [4,5], which allows to obtain a detailed information about the local field, ion-ion, and ion-host interaction processes, or more directly by performing a complete study of the laser emission by pumping with a spectrally narrow tunable source.

Among RE, Neodymium is one of the most investigated ions, not only by reason of its near infrared (IR) emissions, but also because its sensitivity to a changing CF can be used to extrapolate the spectral properties of other RE in similar glass matrices [2]. On the other hand, the study of ion-ion interactions in highly concentrated neodymium materials is a matter of both practical and theoretical importance. High RE concentration allows reducing the size of the gain media and/or the pump power required. However, due to the inherent disorder of glasses, ions in nearby sites may be in physically different environments with greatly varying spectroscopic properties and, as a consequence, spatial migration of energy and spectral diffusion within the inhomogeneously broadened spectral profile [4] can occur. It is worthy noticing that the migration of the electron excitation over the inhomogeneous profile (spectral migration) determines the effectiveness of the stimulated emission generation (amplification) [6] and the wavelength dependence of the laser emission under narrow spectral site-selective pumping.

Nd^{3+}-doped phosphate glasses have been used in high-energy and high-peak-power laser applications for fusion energy research. Among the specific glasses that fulfill the gain, energy storage, extraction efficiency, and damage resistance requirements those based on the P_2O_5-K_2O-MO-Al_2O_3 (MO= MgO, SrO and BaO) composition are reported to be appropriate for large laser amplifiers [7 and references therein]. Although there exists an extensive knowledge about the standard spectroscopic properties of phosphate glasses in relation to laser performance [7,8], no specific study, up to our knowledge, deals with the influence of the host matrix in the spectroscopic and laser properties of Nd^{3+} in a K-Ba-Al phosphate glass as a function of rare earth concentration.

The first part of this investigation presents the fluorescence properties of Nd^{3+} ion as a function of the RE concentration followed by a site-selective and time resolved spectroscopic investigation which includes a detailed analysis of the site-dependent energy diffusion among Nd^{3+} ions by using time resolved fluorescence line narrowing (TRFLN) spectroscopy. The results of this study reveal the influence of crystal field inhomogeneity at the RE sites on the spectral characteristics of the Nd^{3+} spontaneous emission.

The second part deals with the generation of laser action under wavelength selective laser-pulsed pumping. The results confirm the existence of a very complex crystal field site distribution for Nd^{3+} ions producing high sensitivity of the spectroscopic features of the laser

#150021 - $15.00 USD Received 27 Jun 2011; revised 8 Sep 2011; accepted 15 Sep 2011; published 22 Sep 2011

output to the pumping wavelength. In particular, a nonmonotonous dependence of the wavelength of the laser emission peak as well as of the spectral width of the output pulse on the pumping wavelength is observed.

The discussion includes a comparison between the results obtained with site-selective and TRFLN spectroscopy and those obtained in laser generation experiments under tunable wavelength selective pumping which shows the fundamental role played by the crystal field inhomogeneities on the laser behavior of Nd^{3+} ion in this phosphate glass.

2. Materials and experimental spectroscopic techniques

The molar composition of the glasses under study is (62.25-x/2) P_2O_5 + 10 K_2O + (15.5-x/2) BaO + 12.25 Al_2O_3+ x Nd_2O_3, where x ranges from 0.1 to 6 mol%. They were prepared by the conventional melt quenching technique at ambient atmosphere [8] using high purity reagents of $Al(PO_3)_3$, $Ba(PO_3)_2$, KPO_3 and Nd_2O_3 as starting materials. The mixed batches of 30 g were well grounded in an agate mortar and transferred to a platinum crucible and then kept in an electric furnace at around 1050 to 1100° C for 2 h. The molten glasses were poured onto a preheated brass plate and annealed at 350° C for 20 h to remove thermal strains. Finally, the glasses were carefully polished to achieve good optical surfaces.

The density of the glasses was determined by Archimedes´ method using water as the immersion liquid. The refractive index of the samples was determined with an Abbe refractometer using 1-bromonaphthalene as the contact liquid.

The samples temperature was varied between 10 and 300 K in a continuous flow cryostat. Site-selective steady-state emission and excitation spectra were obtained by exciting the samples with a Ti-sapphire ring laser in the 780-920 nm spectral range. The fluorescence was analyzed with a 0.25 m monochromator, and the signal was detected by a Hamamatsu R5509-72 photomultiplier and finally amplified by a standard lock-in technique.

Time resolved resonant fluorescence line narrowed emission measurements were obtained by exciting the samples with a Ti-sapphire laser, pumped by a pulsed frequency doubled Nd:YAG laser (9 ns pulse width), and detecting the emission with a Hamamatsu R5108 photomultiplier provided with a gating circuit designed to enable gate control from an external applied TTL level control signal. Data were processed by an EGG-PAR boxcar integrator.

3. Spectroscopic characterization of Nd^{3+}-doped phosphate glasses

3.1. General fluorescence properties

The $^4F_{3/2}\rightarrow{}^4I_{9/2,11/2}$ steady-state fluorescence spectra were measured at room temperature for all concentrations by exciting with a Ti-sapphire laser at 804 nm in resonance with the $^4I_{9/2}\rightarrow{}^4F_{5/2},{}^2H_{9/2}$ absorption band. Figure 1 shows the emission spectra normalized to the $^4F_{3/2}\rightarrow{}^4I_{11/2}$ emission intensity. Whereas the shape of the emission for the laser transition does not change significantly when increasing concentration, the $^4F_{3/2}\rightarrow{}^4I_{9/2}$ emission shows a different spectral profile as concentration increases due to reabsorption.

As can be seen in Fig. 1, the emission is inhomogeneously broadened due to site-to-site variations in the local ligand field. The fluorescence band for the $^4F_{3/2}\rightarrow{}^4I_{11/2}$ emission was integrated and divided by the peak intensity to yield an effective linewidth [9]. The stimulated emission cross section of the laser transition can be determined from spectral parameters by making use of [9]:

$$\sigma_p\left(\lambda_p\right)=\frac{\lambda_p^4}{8\pi c n^2 \Delta\lambda_{eff}} A\left[\left({}^4F_{3/2}\right);\left({}^4I_{11/2}\right)\right] \qquad (1)$$

where λ_p is the peak fluorescence wavelength, n is the refractive index, $\Delta\lambda_{eff}$ is the effective linewidth of the $^4F_{3/2}\rightarrow{}^4I_{11/2}$ transition, and $A[(^4F_{3/2});(^4I_{11/2})]$ is the radiative transition probability for this transition [8].

#150021 - $15.00 USD Received 27 Jun 2011; revised 8 Sep 2011; accepted 15 Sep 2011; published 22 Sep 2011

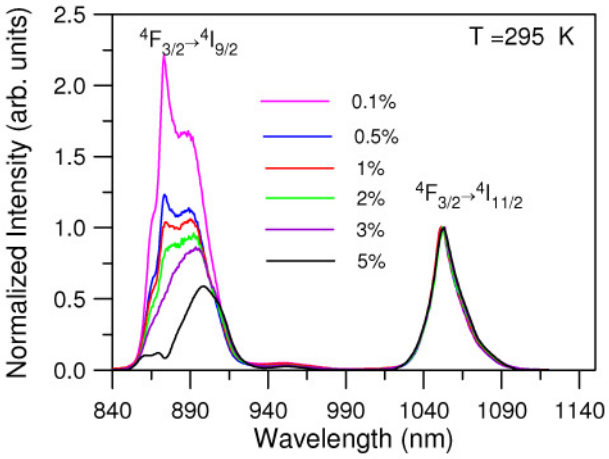

Fig. 1. Room temperature steady-state emission spectra of the $^4F_{3/2}\rightarrow{}^4I_{9/2,11/2}$ transitions for different Nd_2O_3 concentrations.

The stimulated emission cross-section for the $^4F_{3/2}\rightarrow{}^4I_{11/2}$ transition is presented in Table 1 together with the effective fluorescence linewidth ($\Delta\lambda_{eff}$), refractive index (n), peak position (λ_p), and experimental lifetimes (τ_{exp}) measured by exciting at 805 nm with a pulsed (9 ns pulsewidth) Ti-sapphire laser. The values correspond to the fit to a single exponential function.

Table 1. Room temperature emission properties of Nd^{3+} for different concentrations.

Nd_2O_3 (mol%)	n	λ_p(nm)	$\Delta\lambda_{eff}$ (nm)	σ_p (pm^2)	τ_{exp} (μs)
0.1	1.532	1051.5	22.5	7.17	180
0.5	1.533	1051.5	23.0	7.00	170
1	1.534	1052.0	23.6	6.85	130
2	1.536	1052.0	23.4	6.88	100
3	1.538	1052.5	24.4	6.58	90
4	1.538	1052.5	25.0	6.45	75
5	1.547	1052.5	25.0	6.36	45
6	1.550	1053.5	25.5	6.23	40

In order to compare the emission of samples with different Nd^{3+} concentrations, emission measurements were performed in such a way that an absolute comparison could be made among different samples. The following procedure was used: The fluorescence of all samples was excited by using the 488 nm line of a power stabilized argon laser. The samples were cut into slabs and polished to have exactly the same thickness (≈1mm). The pumping radiation was focused into the sample by using a microscope stage with a 0.25 m monochromator and a photomultiplier at the tube end. A low magnifying objective allowed for a close approximation to the upper surface of the sample. To avoid the direct entrance of pumping light into the monochromator, appropriate filters were used. Moreover, the Bertrand lens of the polarizing microscope was also used to slightly misalign the path of the remaining pumping light reaching the entrance slit of the monochromator. The sample was placed so that the spectrometer collected all the luminescence coming from the sample volume contained within the solid angle subtended by the microscope objective. As can be seen in Fig. 2, the integrated emission intensity, corresponding to the $^4F_{3/2}\rightarrow{}^4I_{11/2}$ transition between 1020 and 1120 nm, linearly increases between 0.1 and 4 mol% ($1x10^{21}$ cm^{-3}), and then decreases for the samples doped with 5 and 6% of Nd_2O_3 ($1.27x10^{21}$ and $1.5x10^{21}$ cm^{-3} respectively).

#150021 - $15.00 USD Received 27 Jun 2011; revised 8 Sep 2011; accepted 15 Sep 2011; published 22 Sep 2011

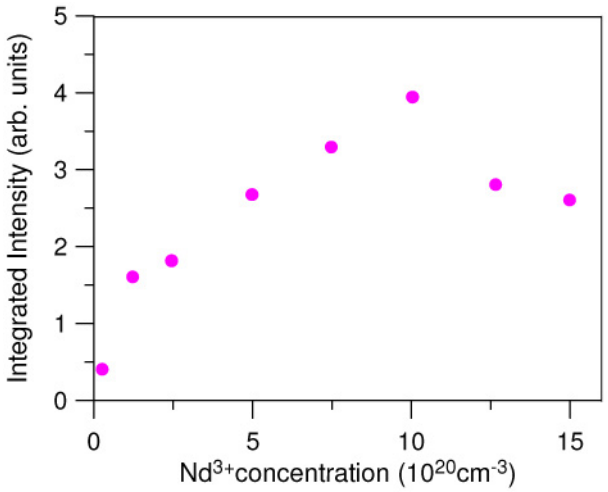

Fig. 2. Integrated emission intensity of the $^4F_{3/2}\rightarrow{}^4I_{11/2}$ transition for different Nd^{3+} concentrations.

3.2. Site-selective spectroscopy

The $^4F_{3/2}\rightarrow{}^4I_{11/2}$ transition of Nd^{3+} ions can show variations in peak wavelength, linewidth, and spectral profile depending on pumping wavelength due to the site-to-site variation of the local field acting on the ions. Therefore, selective excitation of Nd^{3+} by changing the wavelength of the pump laser provides an additional means of varying the gain profile and affecting the laser operation. To understand these processes it is important to investigate the interaction between monochromatic radiation and an assembly of spectrally inhomogeneous active centers.

In order to obtain information about the crystal field site inhomogeneity of Nd^{3+} in these glasses we have performed low temperature site-selective spectroscopy by using a Ti-sapphire ring laser with a narrow bandwidth (0.08 cm^{-1}) as an excitation source for the $^4I_{9/2}\rightarrow{}^4F_{3/2}$ transition. As an example, Fig. 3 shows the excitation spectra of the $^4I_{9/2}\rightarrow{}^4F_{3/2}$ transition obtained by collecting the luminescence at different wavelengths along the $^4F_{3/2}\rightarrow{}^4I_{11/2}$ transition for the sample doped with 0.5 mol%. These spectra show, as expected, two main broad bands associated with the two Stark components of the $^4F_{3/2}$ doublet. However, the low energy component corresponding to the $^4I_{9/2}\rightarrow{}^4F_{3/2}$ doublet, narrows and blue-shifts as the emission wavelength goes from low to high energy. In addition at some emission wavelengths at least two components are observed. This behavior is a consequence of contributions from Nd^{3+} ions in a multiplicity of environments. The monochromatic radiation excites an isochromat corresponding to a subset of sites which may not be physically identical. Therefore, the emission line profile is a composition of emissions from two or more statistical site distributions, which may have different natural homogeneous linewidths.

The site-selective steady-state emission spectra of the laser transition were obtained at low temperature for different excitation wavelengths along the low energy component of the $^4F_{3/2}$ level. As can be observed in Fig. 4 the shape, peak position, and linewidth of the emission band change as excitation goes from high to low energy. The spectra obtained under excitation at the low energy side of the $^4I_{9/2}\rightarrow{}^4F_{3/2}$ absorption band narrow and red shift. The wavelength of the fluorescence peak shifts from 1050 to 1060 nm by varying the excitation wavelength from 871 to 881 nm whereas the effective linewidth is reduced from about 21 nm to 14 nm.

These results show the inhomogeneous behavior of the crystal field felt by Nd^{3+} ions in these glasses. As can be seen in Fig. 4, only when we excite at the high energy side of the absorption band it is possible to cover the full spectral range of the Nd^{3+} emission probably

#150021 - $15.00 USD Received 27 Jun 2011; revised 8 Sep 2011; accepted 15 Sep 2011; published 22 Sep 2011

helped by vibronic transitions. As we shall see in the next section, this behavior is in the origin of the influence of the pumping wavelength on the spectral behavior of the laser emission.

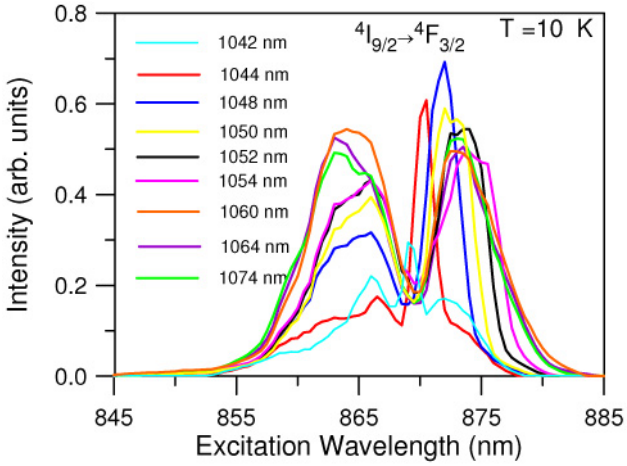

Fig. 3. Excitation spectra of the $^4I_{9/2}\rightarrow{}^4F_{3/2}$ transition obtained by collecting the luminescence at different emission wavelengths along the $^4F_{3/2}\rightarrow{}^4I_{11/2}$ emission for the sample doped with 0.5 mol% of Nd_2O_3. Data correspond to 10 K.

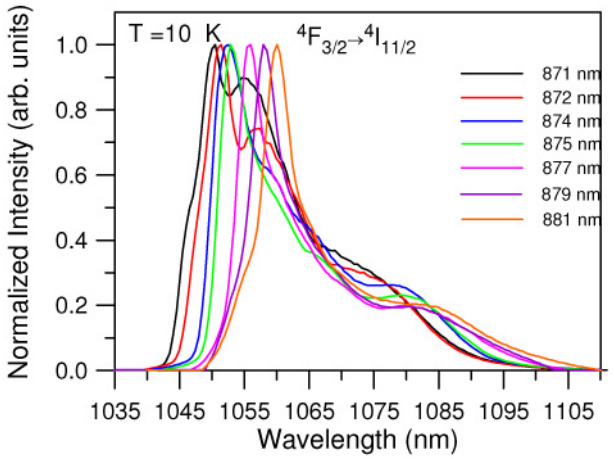

Fig. 4. Steady-state emission spectra of the $^4F_{3/2}\rightarrow{}^4I_{11/2}$ transition for different excitation wavelengths along the low Stark component of the $^4F_{3/2}$ level for the sample doped with 0.5 mol% of Nd_2O_3. Data correspond to 10 K.

3.3. Time-resolved fluorescence line narrowing spectroscopy

As we have mentioned before, the characteristic spectroscopic feature of rare-earth ions in glass is the inhomogeneous broadening which results from the distribution of the crystal fields at the variety of rare-earth ion sites in the amorphous solid. Inhomogeneous broadening substantially influences the lasing processes that occur in the medium. To further investigate the site effects on the luminescence and the energy transfer among Nd^{3+} ions in these glasses we have used TRFLN spectroscopy.

The TRFLN technique provides a way of measuring optical energy propagation from the initially excited subset of ions to other elements of the inhomogeneously broadened line. Therefore, the existence of energy transfer among Nd^{3+} ions in these glasses can be studied by

#150021 - $15.00 USD Received 27 Jun 2011; revised 8 Sep 2011; accepted 15 Sep 2011; published 22 Sep 2011

using TRFLN spectroscopy and observing the emission characteristics of the system as a function of time. The use of tunable lasers for resonant excitation in the near infrared made it possible to perform measurements on TRFLN under resonant excitation of the $^4F_{3/2}$ state of Nd^{3+} in order to study the structure of inhomogeneously broadened bands and migration of excitation energy among Nd^{3+} ions [10 and references therein].

In this technique an inhomogeneously broadened absorption band is excited with a monochromatic laser pulse. Initially, a narrow emission spectrum is observed coming from the ions with an excitation energy which is resonant with the laser. As time increases, in addition to this narrow line, a broad background fluorescence can be observed due to ions excited by energy transfer. The quantity to analyze as a measure of the transfer process is the ratio of the intensity of the narrow line to the total fluorescence intensity in the inhomogeneous line.

We have performed TRFLN spectra at 10 K for the samples doped with 1, 2, 3, and 5% of Nd_2O_3 for the $^4F_{3/2} \rightarrow {}^4I_{9/2}$ transition by exciting at 872 nm in the low energy Stark component of the $^4I_{9/2} \rightarrow {}^4F_{3/2}$ absorption band at different time delays after the laser pulse. Figure 5 shows the spectra obtained at three different time delays after the laser pulse, (a) 5 μs, (b) 100 μs, and (c) 300 μs for the 2% doped sample, where two contributing components are observed. The one on the high energy side of the spectra is an FLN line with a width around 11 cm^{-1}, corresponding to the emission to the lowest Stark component of the ground state. The position of this line is determined by the wavelength of the pumping radiation. In addition to this line we observe a broad nonselected emission. As time delay increases the relative intensity of the narrow line and the broad component changes and the later becomes stronger, which indicates the existence of energy transfer between discrete regions of the inhomogeneous broadened profile. Figure 6 shows the spectra obtained at a time delay of 5 μs for three different concentrations (1, 2, and 5%). As can be observed, at higher concentrations the transfer process appears at shorter time delays and produces a relative increase of the broad emission with respect to the narrow band.

The time evolution of the laser-induced resonant line-narrowed fluorescence is produced by a combination of radiative decay and nonradiative transfer to other nearby ions. Subsequent fluorescence from the acceptor ions replicate the inhomogeneously broadened equilibrium emission profile, showing that transfer occurs not to resonant sites but to the full range of sites within the inhomogeneous profile. In this case, a quantitative measure of the transfer is provided by the ratio of the intensity of the narrow line to the total fluorescence in the inhomogeneous band. Neglecting the dispersion in the radiative decay rate, and using the Föster formula for dipole-dipole energy transfer, one can write for the relation between the integral intensities of the broad background emission I_B and the narrow luminescence component I_N [11]:

$$Ln(1+\frac{I_B}{I_N}) = \gamma(E_L)t^{1/2} \qquad (2)$$

The macroscopic parameter $\gamma(E_L)$ has the meaning of an integral characteristic, which reflects the average rate of excitation transfer from donors to the ensemble of spectrally nonequivalent acceptors [11].

#150021 - $15.00 USD Received 27 Jun 2011; revised 8 Sep 2011; accepted 15 Sep 2011; published 22 Sep 2011

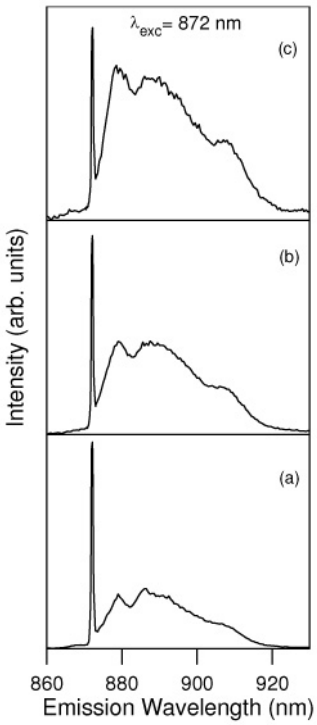

Fig. 5. TRFLN emission spectra obtained at three different time delays after the laser pulse, (a) 5 μs, (b) 100 μs, and (c) 300 μs by exciting at 872 nm for the sample doped with 2% of Nd_2O_3.

#150021 - $15.00 USD Received 27 Jun 2011; revised 8 Sep 2011; accepted 15 Sep 2011; published 22 Sep 2011

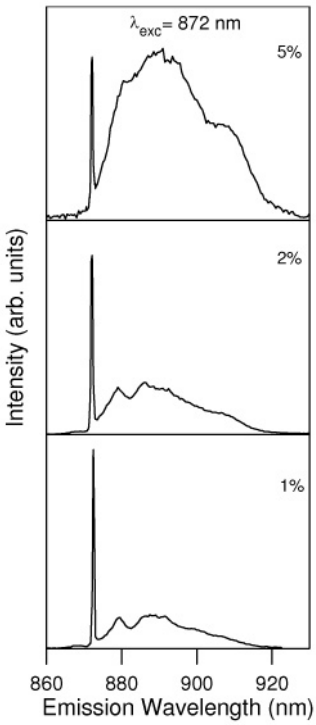

Fig. 6. TRFLN emission spectra obtained at 5 μs by exciting at 872 nm for the samples doped with 1, 2, and 5% of Nd_2O_3.

We have analyzed the TRFLN spectra of the $^4F_{3/2} \rightarrow {}^4I_{9/2}$ transition obtained at different time delays according to Eq. (2) at 10 K. As an example, Fig. 7 shows the results for the samples doped with 1, 2, 3, and 5% obtained by exciting at 872 nm. As can be observed a linear dependence of the $Ln[(I_B/I_N)+1]$ function on $t^{1/2}$ was found, which indicates that a dipole-dipole interaction mechanism among the Nd^{3+} ions dominates in this time regime. The value of the average transfer rate increases from 34 $s^{-1/2}$ to 250 $s^{-1/2}$ when concentration increases from 1 to 5%. This rise in the energy migration rate is due to the increasing number of possible acceptors. The average energy transfer rate found in these glasses is around twice the one found in fluoroarsenate glasses [12] and higher than the one in germanate glasses [13] for a similar concentration of Nd^{3+} ions.

#150021 - $15.00 USD Received 27 Jun 2011; revised 8 Sep 2011; accepted 15 Sep 2011; published 22 Sep 2011

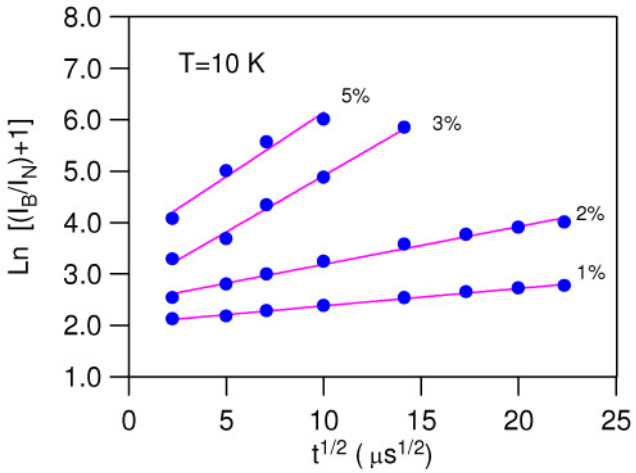

Fig. 7. Analysis of the time evolution of the TRFLN $^4F_{3/2}\rightarrow{}^4I_{9/2}$ emission by means of Eq. (2) for the samples doped with 1, 2, 3, and 5% of Nd_2O_3 Symbols correspond to experimental data and the solid lines are fits to Eq. (2). Data correspond to 10 K.

4. Stimulated emission experiments under wavelength selective pumping

4.1 Laser performance and sample parameters

Laser dynamics experiments were performed by pumping the Nd-doped slabs with 9 ns pulses of a tunable Ti-sapphire pulsed laser at wavelengths inside the $^4I_{9/2}\rightarrow{}^4F_{5/2}$ absorption band of Nd^{3+} ions. The samples were placed in a 15 cm long confocal resonator and oriented at Brewster angle to minimize the intra-cavity losses. The pump beam was slightly focused on the sample in such a way that the pumped area was 3 mm^2. The spectra of the output laser pulses, after filtering the pumping residual signal and diffusing, were recorded with a diode-array Hamamatsu-Triax 190 spectrum analyzer using a 600 lines/mm diffraction grating. The temporal evolution of both pumping and laser output pulses was recorded with a fast photodiode connected to a digital oscilloscope.

We have studied eight different sample plates with different thicknesses and concentrations (0.1-6% Nd_2O_3). Although the apparent optical qualities were similar, we made a careful study of the optical losses of all the investigated samples in order to compare optical qualities and laser efficiencies. In fact we tried to relate passive losses, pump energy absorption of the samples, and lasing threshold energy.

The population inversion can be calculated from $N(x)=\alpha E\exp(-\alpha x)$, where x is the longitudinal coordinate along the sample, α the absorption coefficient, and E the incident photon number per pulse and unit area, obtained from the incident pump energy, pumped sample area, and pump photon energy. The amplification of the stimulated radiation is given by the following expression $\frac{dI(x)}{dx}=\sigma I(x)N(x)$, where $I(x)$ is the intensity of the stimulated radiation and σ is the stimulated emission cross-section. The gain is obtained from an intensity integration throughout the sample and given by: $Ln(G)=\sigma E\left[1-\exp(-\alpha d)\right]$, where d is the sample thickness. The threshold condition is $G>1/T$, being T the passive transmittance of the sample, which is related to the passive optical density, $D_0=-0.43Ln(T)$. On the other hand, the absorption term is related to the optical density at maximal absorption wavelength, $D=0.43\alpha d$. So, the relation between D, σ, and the optical density referred to the passive optical losses D_0 at threshold is:

#150021 - $15.00 USD Received 27 Jun 2011; revised 8 Sep 2011; accepted 15 Sep 2011; published 22 Sep 2011

$$D_0 = 0.43 E_{th} \sigma (1 - 10^{-D}) \quad (3)$$

where E_{th} is the incident pump photon number per pulse and unit sample area just at laser threshold (using both HR mirrors).

Table 2 presents the experimental results obtained for all the samples with different Nd^{3+} ion concentrations. The passive density data D_0 show the very different optical qualities of the samples studied; these differences are due to the growth and doping processes, because the surface treatment improved quality to be similar in all cases. The absorption density D depends on the absorption coefficient α, and therefore on ion concentration, and it is obviously influenced by the thickness d of the samples. The absorption coefficients are in good agreement with the nominal Nd_2O_3 concentrations.

It is worth noticing that to be useful for laser applications a good sample must fulfil the conditions of enough absorption and low optical passive losses. Account taken of the results shown in Table 2 it is clear that both conditions are best accomplished in the sample of 5% concentration where high absorption of the pump radiation (with no need of higher thickness) due to its high concentration and above all, a very good optical quality concur. This sample was tested by using output couplers of different reflectivities. The most adequate for working at the maximum available pumping energy (about 40 mJ absorbed) was the one with a reflectivity R = 60%. With this output coupler the absorbed pump energy at threshold was 18 mJ, and the maximum output energy obtained 9 mJ, being the slope efficiency of about 40%. All the rest of samples were also tested, and showed lower performances.

Table 2. Laser threshold pump energy and passive losses for different samples. *D* is the optical density at maximal absorption wavelength (799 nm), E_{th} is the laser threshold pump energy, D_0 is the optical density due only to passive losses obtained from Eq. (3), and *d* is the sample thickness.

Nd_2O_3 (mol%)	0.1%	0.5%	1%	2%	3%	4%	5%	6%
D	0.20	0.43	0.65	1.27	1.93	2.03	1.58	2.56
E_{th} *(mJ)*	>40	5	15	20	30	40	<1	10
D_0	>0.06	0.012	0.05	0.08	0.11	0.17	<0.004	0.04
d (mm)	7.8	3.3	3.0	2.8	2.9	2.2	1.2	2.0

4.2 Pumping wavelength dependence of the laser spectra

The averaged laser output spectra were recorded as a function of pumping wavelength along the $^4I_{9/2} \rightarrow {}^4F_{5/2}$ absorption band. Figure 8 shows a 3D picture of the laser (excitation/emission) spectrum obtained from the 5% Nd_2O_3-doped sample, that is, the laser output spectrum as a function of excitation wavelength. As can be seen, due to the absorption profile of the $^4I_{9/2} \rightarrow {}^4F_{5/2}$ absorption band the laser emission has a maximum output intensity when pumped between 794 and 804 nm. On the other hand, the emission spectrum is relatively broad (FWHM ~3nm) and presents an irregular energy distribution around the absorption wavelength maximum (799 nm), and moreover the peak of the output spectra slightly shifts in the pumping wavelength interval. As an example Fig. 9 shows three series of emission spectra obtained at different excitation wavelengths. In all the samples studied, the lowest emission peak wavelength, situated between 1053 and 1054 nm, depending on the concentration of the sample, was obtained by exciting around 800 nm, just when the laser emission intensity was maximum. For longer pumping wavelengths, up to 806-7 nm, the wavelength of the emission peak shifts towards longer wavelengths, between 1055 and 1057 nm, depending on sample concentration. This shift is greater at high concentrations (up to 3 nm in the 6% Nd_2O_3-doped sample) than at low concentrations (about 1 nm at 1%), and it is possible to find some spectral structure in this transition zone (see Fig. 9). The spectral shift is also a little greater at high pumping energies than at low ones. However, for excitation wavelengths longer than 807 nm, the wavelength of the emission peak slightly shifts again to shorter wavelengths.

On the other hand, the spectral width of the laser emission is observed to get wider as the concentration and pumping energy increase (FWHM varies from 1.5 to 2 nm in the 0.5%

#150021 - $15.00 USD Received 27 Jun 2011; revised 8 Sep 2011; accepted 15 Sep 2011; published 22 Sep 2011

Nd_2O_3-doped sample and up to 2.5 nm in the 6% Nd_2O_3-doped one), showing the high crystal field inhomogeneity of the glass matrix as well as the influence that concentration exerts upon it.

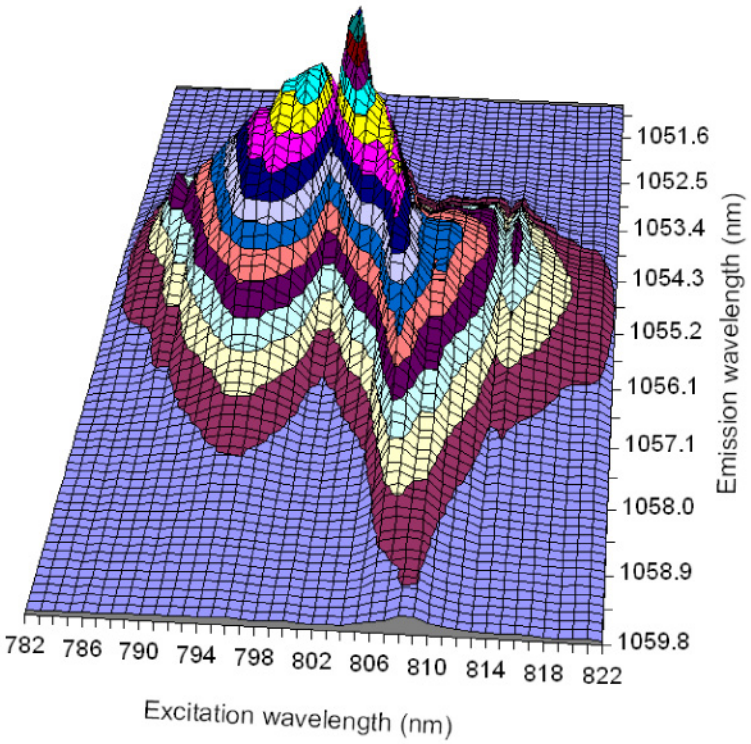

Fig. 8. Laser output spectra of $^4F_{3/2} \rightarrow {}^4I_{11/2}$ transition for the sample doped with 5 mol% as a function of excitation wavelength along the $^4F_{5/2}$ level.

#150021 - $15.00 USD Received 27 Jun 2011; revised 8 Sep 2011; accepted 15 Sep 2011; published 22 Sep 2011

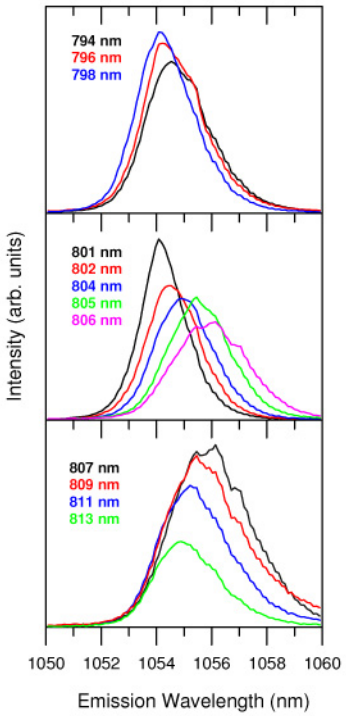

Fig. 9. Laser output spectra of $^4F_{3/2} \rightarrow {}^4I_{11/2}$ transition as a function of excitation wavelength for the sample doped with 5 mol%.

5. Discussion

The results obtained in sections 3 and 4 point out to a close relation between the site effects produced by changes in the ligand environment around the RE and the spectral behavior of laser emission in the studied phosphate glasses. It is clear that in spite of the amorphous character of the glass matrix there is still a high degree of local order determined by the structure and symmetry of the crystal field felt by Nd^{3+} ion. It is worthy mentioning that the spectral response of the RE under wavelength selective excitation follows similar trends to those of the spectral behavior of the stimulated emission under wavelength selective pumping. In particular, the displacement ranges of the emission peaks of both spontaneous and stimulated emissions as a function of excitation wavelength shown in Figs. 4 and 9 are within the same order of magnitude though, obviously, the red shift of the laser emission peak occurs in a shorter range due to gain limitations. On the other hand, the site-selective spontaneous emission measured by exciting in the low energy component of the $^4F_{3/2}$ level presents strong profile changes and narrowing when the excitation wavelength increases, which indicates the presence of a complex variety of emitting centers. Moreover, the observed narrowing and shifts in the excitation spectra of $^4F_{3/2}$ level as a function of collecting wavelengths, shown in Fig. 3, can be compared to the laser excitation spectra profiles presented in Fig. 10, and obtained by collecting the laser emission at the short and long wings of the laser spectrum. As can be seen, both figures suggest the existence of well defined inhomogeneous RE site distributions. The persistence of this inhomogeneous behavior in the laser emission at room temperature in heavy RE-doped samples means that ion-ion energy transfer is not very efficient, at least during the build up time of the laser pulse, because, as we mentioned in subsection 3.3, in addition to causing a spatial migration of energy, it may also produce spectral diffusion within the inhomogeneously broadened spectral profile. This hypothesis is confirmed by the average transfer rates given by TRFLN measurements in these glasses (subsection 3.3), which though a little higher than in fluoroarsenate [12], and germanate

#150021 - $15.00 USD Received 27 Jun 2011; revised 8 Sep 2011; accepted 15 Sep 2011; published 22 Sep 2011

glasses [13] are not high enough to equalize the energy differences of these broad site distributions of Nd^{3+} ions in these phosphate glasses.

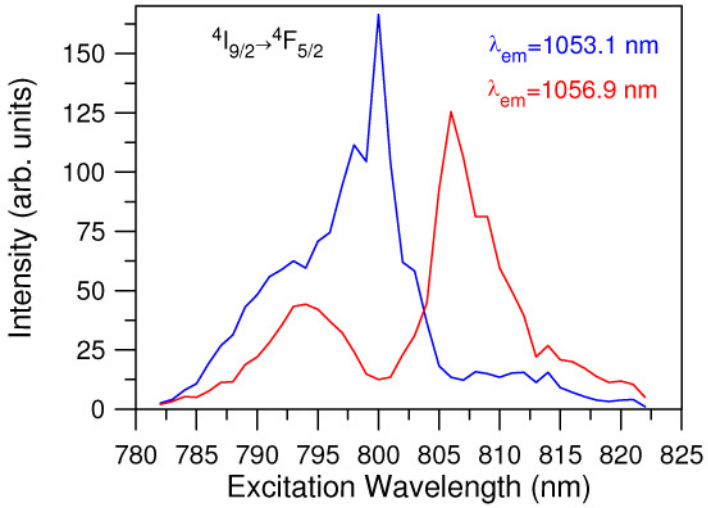

Fig. 10. Laser excitation spectra profiles obtained by collecting the laser emission at short and long wings of the laser spectrum transition for the sample doped with 5 mol%.

6. Summary and conclusions

We have investigated the spectroscopic features of the spontaneous and stimulated emissions of Nd^{3+} ions in a K-Ba-Al phosphate glass. The study points out the importance of wavelength selective excitation in order to understand the influence of matrix inhomogeneity on the laser performance of a material and therefore the possibility of controlling its benefits and/or drawbacks.

Heavy Nd^{3+}-doped samples have been probed to be efficient laser emitters in this phosphate matrix. The highest laser efficiency was obtained in a 5% Nd_2O_3- doped sample by pumping near the wavelength maximum of the $^4I_{9/2}\rightarrow{}^4F_{5/2}$ absorption band. The obtained laser slope is about 40%.

As a consequence of the crystal field inhomogeneity produced by the glass matrix the spectral width as well as the peak position of the emitted laser pulses depend on the wavelength and energy of the pump pulse. These matrix characteristics could allow for some spectral tuning of the laser output pulse and opens the possibility of exercising some control over the output laser wavelength by manipulating the glass composition.

Acknowledgments

This work has been supported by the Spanish Government under Projects No. MAT2008-05921/MAT, MAT2009-14282-C02-02, FIS2011-27968, Consolider SAUUL CSD2007-00013, and Basque Country Government (IT-331-07). One of the authors (CKJ) is grateful to DAE-BRNS, Govt. of India, Mumbai for the sanction of major research project (No.2007/34/25-BRNS/2415, dt.18-01-2008).

#150021 - $15.00 USD Received 27 Jun 2011; revised 8 Sep 2011; accepted 15 Sep 2011; published 22 Sep 2011